Diagn Interv Radiol 2022; DOI 10.5152/dir.2022.20783

ABDOMINAL IMAGING

ORIGINAL ARTICLE

A new proposal of an ultrasonic imaging model for predicting overall and progression-free survival in patients with primary hepatocellular carcinoma

Xiao-Yun Li
Lin-Lin Wang

PURPOSE
We aimed to develop models for predicting overall survival (OS) and progression-free survival (PFS) of patients with primary hepatocellular carcinoma (HCC).

METHODS
Clinicopathological characteristics and laboratory information of patients were collected. We retrospectively analyzed presurgical data of 216 patients with primary HCC. The random forest and least absolute shrinkage and selection operator regression models were used to select features. We established prognostic models for predicting OS and PFS of primary liver cancer using ultrasonic imaging as well as clinical and pathological features. Accuracy of the models was evaluated using area under the curve, C index, and calibration curves, whereas their clinical application value was assessed using decision curve analysis.

RESULTS
Models for predicting OS and PFS were established based on ultrasonic imaging accessible features. The models showed excellent accuracy and prognosis prediction of OS and PFS in patients with primary HCC.

CONCLUSION
The established models based on factors such as aspartate aminotransferase platelet ratio index, Child-Turcotte-Pugh grade, tumor grade, hepatitis B virus-DNA, the intensity of ultrasound enhancement at the portal stage, lymphocyte/monocyte ratio, portal hypertension, gender, stage, the beginning time of ultrasonic contrast, and the total grade of ultrasonic enhancement can effectively predict OS and PFS of primary HCC.

Primary liver cancer (PLC) is the fourth leading cause of cancer-related deaths worldwide.[1] Previous studies have shown that PLC results from abnormal proliferation of new blood vessels in cancer tissues, which promote proliferation of cancer cells and tissue infiltration.[2] Therefore, analysis of blood flow signals in a patient's liver is vital during analysis of tumor biology and prognostic evaluation.[3] Advancements in imaging technology and contrast-enhanced ultrasound have improved the clinical evaluation of hemodynamics of PLC.[3] Previous studies have mainly analyzed differences in ultrasound imaging echoes of patients and quantitative analyses have not been performed.[4] Despite using computer image recognition technology to extract key features in tumor images to achieve prognosis prediction, the technology is often difficult to apply in the current clinical practice.[5] Therefore, it is imperative to develop an easy-to-use visual prediction model for accurate and effective prognosis of PLC.

Numerous studies have reported the important role of chronic inflammation on the proliferation, angiogenesis, and immunosuppression of cancer cells.[6] For example, cancer-related inflammation (CRI) has been associated with poor cancer prognosis.[7,8] In fact, clinical features of CRI including lymphocyte/monocyte ratio (LMR), aspartate aminotransferase platelet ratio index (APRI), and neutrophil-to-lymphocyte ratio (NLR) have been widely used for the treatment and prognosis of cancer. These noninvasive biomarkers can be easily detected. Furthermore, new important features such as liver and spleen stiffness have also been demonstrated to be reliable noninvasive tests for predicting primary

From the Department of Ultrasound (X.Y.L.), Shangluo Central Hospital, ShaanxiPeople's Republic of China; Department of Ultrasound (L.L.W. WangLinlinLC@outlook.com), Xianyang Maternal and Child Health Hospital, Shaanxi; People's Republic of China.

Received 3 October 2020; revision requested 24 November 2020; last revision received 8 April 2021; accepted 15 April 2021.

Available online: 14 June 2022.

DOI: 10.5152/dir.2022.20783

You may cite this article as: Li X-Y, Wang L-L. A new proposal of an ultrasonic imaging model for predicting overall and progression-free survival in patients with primary hepatocellular carcinoma. *Diagn Interv Radiol.* 2022;28(4):301-311.

hepatocellular carcinoma (HCC) occurrence, as can be observed in previous research.[9,10] These studies provide valuable insights into the screening of predictors to build a valid predictive model.

The present study used the prevailing literature on liver ultrasound contrast characteristics and related parameters to establish a model for predicting the overall survival (OS) and progression-free survival (PFS) of patients with primary HCC. The factors included in the models were patient's general condition, CRI-related characteristics, and tumor biological characteristics. We hypothesized that based on these characteristic factors, a nomogram for effective and early prediction of OS and PFS in patients with primary HCC can be established.

Methods

Study subjects, inclusion, and exclusion criteria

This retrospective study was approved by the ethics committee of (approval no. 2018004), and was conducted in accordance with the Helsinki Declaration. We enrolled patients who were treated for primary HCC from July 2016 to July 2020. All enrolled subjects lived in China and were expected to provide informed consent prior to inclusion in the study. All patients underwent contrast-enhanced ultrasound examination before surgery. The final diagnosis of all 216 patients was based on the histopathological results of intraoperative liver biopsy. The exclusion criteria were patients who lacked important pathological results; poor imaging quality results; patients with systemic infections; those who manifested severely inadequate heart, liver, and kidney function; patients with other major diseases; those with a preoperative liver function of Child-Pugh C; patients who had been treated for other liver cancer before admission; and those who were unwilling to participate in the study. A summary of the patients' characteristics, including their gender and age, is outlined in Table 1. OS and PFS were defined as the points.

Parameters

Venous blood samples were collected on the day of the biopsy and used for hematological analysis, including blood cell count and quantification of the following factors: alpha-fetal protein (AFP), APRI; the LMR, NLR, platelet-to-lymphocyte ratio (PLR), and the presence of hepatitis B virus (HBV)-DNA in liver biopsies of patients with hepatitis B. All biochemical analyses were performed using standard laboratory methods, and the corresponding biologically effective dose (BED10) was calculated.

Ultrasound examination

Imaging examination was performed using GE Logiq E9 (GE Healthcare) and iU22 scanner (Philips Healthcare), with a probe frequency set to 2-5 MHz. Briefly, sulfur hexafluoride was first dissolved in 5 mL of 0.9% normal saline, and then 0.04 mL/kg was injected through the cubital vein. During the examination, liver and tumor nodules were subjected to regular 2-dimensional grayscale and color Doppler scans, followed by injection of the aforementioned contrast agents. The collected ultrasound features include the intensity of ultrasound enhancement at arterial phase, intensity of ultrasound enhancement at portal stage, intensity of ultrasound enhancement at delayed phase, the beginning time of ultrasonic contrast, peak time of ultrasonic contrast, and attenuation time of ultrasonic contrast.

A timer was started during blousing of the contrast agent while the ultrasonic mechanical index was constant during the inspection. The probe was fixed into position, and the patient was asked to breathe calmly to ensure the stability of the scanning plane. Imaging diagnosis was exclusively performed by the same 2 doctors, during which the beginning, peak, and attenuation times of ultrasonic contrast were recorded. Utmost care was taken when using these valuable pieces of equipment, and no major modifications or re-settings were made to the ultrasound machinery. After injection of the contrast agent, 0-30, 30-120, and 121-360 s periods representing the arterial, portal, and delayed phases, respectively, were allowed. It should be added that the identification of these 3 periods also refers to both the EFSUMB guidelines and previous studies.[11–13] HYPER-HYPO: Arterial hyperenhancement and definite hypoenhancement compared to portal and/or late peripheral parenchyma; ISO-ISO: Same as surrounding parenchymal enhancement; HYPER-ISO: Arterial hyperenhancement, portal/late-stage identical to peripheral parenchymal enhancement.

The region of interest was placed at the HCC tissue and normal liver tissue adjacent to the cancer, and the peak intensity (PI) and basic intensity (BI) of the curves were recorded. As for the enhanced intensity (EI), EI (dB) = PI (dB) – BI (dB). The intensity of ultrasound enhancement was divided into low, medium, and high enhancement according to the ratio of 3 : 2 : 5 in order to make the study more widely applied.[14] Thus, the ultrasound intensity in different phases was defined as low, medium, and high enhancement according to the EI. Low enhancement was scored as 0, medium enhancement as 1, and high enhancement as 2. Then, the total grade of ultrasonic enhancement was obtained by summing the ultrasonic intensity of the arterial phase, portal phase, and delayed phase of the same patient.

Feature selection, establishment of a prediction model, and statistical analysis

A total of 25 feature factors were selected, after which feature selection was performed using the randomForestSRC software package. The randomSurvivalForest algorithm was utilized to rank the importance of prognostic-related genes. Specifically, we used n_{rep} = 100, which indicates that the number of iterations in the Monte Carlo simulation was 100, and n_{step} = 5, which indicates that the number of steps forward was 5. Based on this, 24 features were found to be OS-related signatures in the liver. Next, we incorporated the 24 factors into the least absolute shrinkage and selection operator (LASSO) analysis for reduction of data dimensionality and screened out suitable predictors as previously described.[15–19] The 5 cross-validation method was chosen to obtain the optimal parameters in the LASSO model. We randomly sampled the training and validation sets, at a ratio of 7 : 3. The training queue was used to select features and generate predictive models as previously described.[20] Furthermore, multivariate Cox regression models were used to build models for predicting the risk of recurrence and death caused by primary HCC[21,22] and generated calibration curves to evaluate model accuracy.[23] To assess the performance of the nomogram, we used R software packages to measure the C index and the area under the curve (AUC), and this was conducted repeatedly to verify the nomogram (10 000 repeated samples).[23,24] The Cox regression models presented in Tables 2 and 3 are the parameters of the Cox regression models in

Table 1. Basic characteristics of patients

Variable	Total (n = 216)	Progression-free survival: Recurrence (n = 156)	Progression-free survival: No recurrence (n = 60)	*P*	Overall survival: Dead (n = 114)	Overall survival: Alive (n = 102)	*P*
Survival (months), mean ± SD	44.8 ± 13.8	42.2 ± 13.3	51.7 ± 12.6	<0.001	40 ± 12.9	50.2 ± 12.7	<0.001
Age (years), mean ± SD	58.3 ± 11.8	57.4 ± 12.1	60.5 ± 10.8	0.0089	57.2 ± 12.7	59.5 ± 10.7	0.151
Male sex, n (%)	183 [84.7]	138 [63.9]	45 [75]	0.014	102 [89.5]	81 [79.4]	0.040
Tumor size (mm), mean ± SD	34 ± 13.6	32.7 ± 13.6	37.6 ± 12.8	0.018	32.8 ± 14	35.5 ± 13	0.144
Tumor grade, n (%)				0.002			<0.001
I	51 [23.6]	27 [12.5]	24 [40]		9 [7.9]	42 [41.2]	
II	108 [50]	81 [37.5]	27 [45]		60 [52.6]	48 [47]	
III	51 [23.6]	42 [19.4]	9 [15]		39 [34.2]	12 [11.8]	
IV	6 [2.8]	6 [2.8]	0 [0]		6 [5.3]	0 [0]	
Stage, n (%)				<0.001			<0.001
I	128 [59.2]	68 [31.5]	60 [100]		30 [26.3]	98 [96.1]	
II	36 [16.7]	36 [16.7]	0 [0]		33 [29]	3 [2.9]	
III	52 [24.1]	52 [24.1]	0 [0]		51 [44.7]	1 [1]	
T, n (%)				<0.001			<0.001
T1	155 [71.8]	95 [44]	60 [100]		57 [50]	98 [96.1]	
T2	61 [28.2]	61 [28.2]	0 [0]		57 [50]	4 [3.9]	
M, n (%)				0.279			0.099
M0	213 [98.6]	153 [70.8]	60 [100]		111 [97.4]	102 [100]	
M1	3 [1.4]	3 [1.4]	0 [0]		3 [2.6]	0 [0]	
Scope regional lymph nodes removed in surgery, n (%)				0.557			0.055
No regional lymph nodes removed	3 [1.4]	3 [1.4]	0 [0]		3 [2.6]	0 [0]	
1 to 3 regional lymph nodes removed	192 [88.9]	138 [63.9]	54 [90]		96 [84.2]	96 [94.1]	
4 or more regional lymph nodes removed	21 [9.7]	15 [6.9]	6 [10]		15 [13.]	6 [5.9]	
Total number of tumors for patient, n (%)				0.001			<0.001
One	174 [80.6]	117 [54.2]	57 [95]		78 [68.4]	96 [94.1]	
More than one	42 [19.4]	39 [18.1]	3 [5]		36 [31.6]	6 [5.9]	
CTP grade, n (%)				0.491			0.005
CTPA	189 [87.5]	135 [62.5]	54 [90]		93 [81.6]	96 [94.1]	
CTPB	27 [12.5]	21 [9.7]	6 [10]		21 [18.4]	6 [5.9]	
HBV-DNA, n (%)				0.048			0.333
Negative	126 [58.3]	87 [40.3]	39 [65]		63 [55.3]	63 [61.8]	
Positive	90 [41.7]	69 [31.9]	21 [35]		51 [44.7]	39 [38.2]	
APRI, n (%)				0.001			0.001
<0.47	122 [56.5]	77 [35.6]	45 [75]		49 [43]	73 [71.6]	
≥0.47	94 [43.5]	79 [36.6]	15 [25]		65 [57]	29 [28.4]	
BED10 (Gy), n (%)				0.538			0.333
<100	90 [41.7%]	63 [29.2]	27 [45]		51 [44.7]	39 [38.2]	
≥100	126 [58.3]	93 [43.1]	33 [55]		63 [55.3]	63 [61.8]	
AFP (ng/mL), n (%)				0.009			0.026
<400	156 [72.2]	105 [48.6]	51 [85]		75 [65.8]	81 [79.4]	
≥400	60 [27.8]	51 [23.6]	9 [15]		39 [34.2]	21 [20.6]	

Table 1. Basic characteristics of patients (Continued)

Variable	Total (n = 216)	Progression-free survival: Recurrence (n = 156)	Progression-free survival: No recurrence (n = 60)	*P*	Overall survival: Dead (n = 114)	Overall survival: Alive (n = 102)	*P*
NLR, mean ± SD	2.1 ± 1	2.2 ± 1	2.1 ± 1	0.583	2.2 ± 1.1	2 ± 0.9	0.108
PLR, mean ± SD	108.2 ± 47.6	105.3 ± 45.2	115.8 ± 53	0.148	102.2 ± 44.3	115 ± 50.4	0.048
LMR, mean ± SD	3.6 ± 1.3	3.6 ± 1.2	3.5 ± 1.4	0.620	3.5 ± 1.2	3.7 ± 1.3	0.376
Portal hypertension, n (%)				0.015			0.036
Absent	171 [79.2]	117 [54.2]	54 [90]		84 [73.7]	87 [85.3]	
Present	45 [20.8]	39 [18.1]	6 [10]		30 [26.3]	15 [14.7]	
Intensity of ultrasound enhancement at arterial phase				0.616			0.074
Low	191 [88.4]	139 [64.4]	52 [86.7]		105 [92.1]	86 [84.3]	
Medium	25 [11.6]	17 [7.9]	8 [13.3%		9 [7.9]	16 [15.7]	
Intensity of ultrasound enhancement at portal phase, n (%				<0.001			<0.001
Low	11 [5.1]	5 [2.3]	6 [10]		0 [0]	11 [10.8]	
Medium	70 [32.4]	37 [17.1]	33 [55]		13 [11.4]	57 [55.9]	
High	135 [62.5]	114 [52.8]	21 [35]		101 [88.6]	34 [33.3]	
Intensity of ultrasound enhancement at delayed phase, n (%)				0.002			<0.001
Low	2 [0.9]	2 [0.9]	0 [0]		0 [0]	2 [2]	
Medium	22 [10.2]	9 [4.2]	13 [21.7]		0 [0]	22 [21.6]	
High	192 [88.9]	145 [67.1]	47 [78.3]		114 [100]	78 [76.4]	
Total grade of ultrasonic enhancement, n (%)				<0.001			<0.001
0	2 [0.9]	2 [0.9]	0 [0]		0 [0]	2 [2]	
1	5 [2.3]	3 [1.4]	2 [3.3]		0 [0]	5 [4.9]	
2	28 [13]	10 [4.6]	18 [30]		0 [0]	28 [27.4]	
3	64 [29.6]	40 [18.5]	24 [40]		22 [19.3]	42 [41.2]	
4	117 [54.2]	101 [46.8]	16 [26.7]		92 [80.7]	25 [24.5]	
The beginning time of ultrasonic contrast (seconds), mean ± SD	13 ± 3	12.9 ± 2.9	13.2 ± 3.3	0.455	12.6 ± 2.9	13.4 ± 3.1	0.037
Peak time of ultrasonic contrast (seconds)	44.7 ± 17.2	44.1 ± 17.1	46.5 ± 17.7	0.364	43.7 ± 18	45.9 ± 16.4	0.348
Attenuation time of ultrasonic contrast (seconds), mean ± SD	92 ± 61.4	83 ± 53.7	115.2 ± 73.4	<0.001	71.9 ± 43.6	114.4 ± 70.2	<0.001

AFP, alpha-fetal protein; APRI, aspartate aminotransferase platelet ratio index; BED10, biologically effective dose; CTP, Child-Turcotte-Pugh; LMR, lymphocyte/monocyte ratio; NLR, neutrophil-to-lymphocyte ratio; PLR, platelet-to-lymphocyte ratio.

Figures 3a, 4d, respectively. Therefore, the proportional hazards, assumptions, and the evaluation of the model fit for the Cox regression models in Tables 2 and 3 were done by calculating the C index (Figures 3c, 3d) and plotting the receiver operating characteristic (ROC) curves (Figures 4f, 4g) for the training and validation groups, respectively. The clinical utility of the nomogram was determined using decision curve analysis (DCA) as previously described.[25] In short, DCA is used to quantify the net benefit of different threshold probabilities in patient information and thus assess the rate of treatment benefit for patients. All statistical tests were 2-sided; $P < .05$ was considered statistically significant. Descriptive statistics are presented as mean ± standard deviation (SD) of the mean. The study was conducted in accordance with the guidelines of the Transparent Reporting of a Multivariate Prediction Model for Individual Prediction or Diagnosis.[26] All statistical analyses were performed in R software (version 3.5.4).

Results

In total, 216 patients with primary HCC, with an average age of 61 ± 11.8 years, were enrolled in the study. Among them, 183 were male patients and 33 female patients. During the follow-up period, 114 (52.8%) patients succumbed to liver cancer, whereas 156 (72.2%) manifested tumor recurrence. The overall characteristics of the

Table 2. Multivariable Cox model of overall survival for primary hepatic carcinomas using clinical and ultrasonic features

	Overall survival	
Variables	HR (95% CI)	*P*
Female sex	0.289 (0.145-0.573)	<0.001
Tumor grade	3.312 (2.479-4.425)	<0.001
Stage	2.941 (2.352-3.676)	<0.001
CTP grade	2.12 (1.313-3.424)	0.002
HBV-DNA	1.575 (1.078-2.299)	0.019
APRI ≥ 0.47	2.096 (1.435-3.061)	<0.001
LMR	0.939 (0.819-1.077)	0.370
Portal hypertension	1.556 (1.016-2.382)	0.042
The beginning time of ultrasonic contrast	0.907 (0.852-0.966)	0.003
Intensity of ultrasound enhancement at portal stage	7.378 (4.154-13.104)	<0.001
Total grade of ultrasonic enhancement	5.527 (3.529-8.656)	<0.001

HR, hazard ratio; CI, confidence interval; CTP, Child-Turcotte-Pugh; HBV, hepatitis B virus; APRI, aspartate aminotransferase platelet ratio index; LMR, lymphocyte/monocyte ratio.

Table 3. Multivariable Cox model of progression-free survival for primary hepatic carcinomas using clinical and ultrasonic features

	Progression-free survival	
Variables	HR (95% CI)	*P*
Gender, female	0.402 (0.245-0.66)	<0.001
Tumor grade	2.209 (1.738-2.806)	<0.001
Stage	2.008 (1.675-2.408)	<0.001
CTP grade	1.282 (0.802-2.048)	0.299
HBV-DNA	1.547 (1.119-2.138)	0.008
APRI ≥ 0.47	1.507 (1.1-2.066)	0.011
LMR	0.958 (0.873-1.045)	0.397
Portal hypertension	1.364 (0.942-1.974)	0.100
The beginning time of ultrasonic contrast	0.937 (0.889-0.988)	0.016
Intensity of ultrasound enhancement at portal stage	2.628 (1.892-3.649)	<0.001
Total grade of ultrasonic enhancement	2.012 (1.585-2.554)	<0.001

HR, hazard ratio; CI, confidence interval; CTP, Child-Turcotte-Pugh; HBV, hepatitis B virus; APRI, aspartate aminotransferase platelet ratio index; LMR, lymphocyte/monocyte ratio.

study population are summarized in Table 1. In addition, we recommend that readers pay due attention to the figures and tables, which are exhaustive and facilitate understanding of the analyses conducted in the cohort study.

Here, the randomForestSRC R software package allowed successful feature selection. The relationship between the error rate and some classification trees is depicted in Figure 1a, while the order of the out-of-bag importance of those features is shown in Figure 1b. To prevent the overfitting of the predictive model, we modeled the characteristic factors obtained in the above process using the LASSO-penalized multivariate Cox proportional hazards model. In particular, we randomly performed 1000 LASSO regressions and then incorporated them into the Cox regression model based on the number of occurrences of predictors, followed by the calculation of their AUC values in order to obtain the best combination of predictors. Our findings revealed that a total of 11 predictive factors, namely, APRI, Child-Turcotte-Pugh (CTP) grade, tumor grade, HBV-DNA, the intensity of ultrasound enhancement at the portal stage, LMR, portal hypertension, gender, stage, the beginning time of ultrasonic contrast, and total grade of ultrasonic enhancement were used in model construction (Figure 1c, 1d). Finally, the Kaplan-Meier curves demonstrated that the resulting prediction model was effective in classifying the poor survival rates of the patients ($P < .001$) (Figure 1e).

Based on the 11 characteristic factors selected using LASSO analysis, a principal component analysis (PCA) stratified the population for prediction of the survival rate of the patients (Figure 2a). The distribution of the prognostic index in this cohort is displayed in Figure 2b, while the OS prognosis of patients in high/low-risk groups is illustrated in Figure 2c. We observed that in the high-risk group, the 5-year survival rate of patients was only 10%, which was significantly lower than the 82% observed in the low-risk group. Furthermore, the 5-year survival rate in the high-risk group increased from 10% at 2 years to 20% and 40% in 3 and 4 years, respectively, after surgery (Figure 2d). On the other hand, the 5-year survival rate in the low-risk group increased from 82% at 2 years to 84% and 88% in 3 and 4 years, respectively, after surgery (Figure 2e). Taken together, these outcomes imply that the prognostic model, based on the 11 characteristics, can effectively stratify patient prognosis.

To construct a nomogram for predicting OS in primary HCC patients, we randomly divided the study cohort into training and validation sets (ratio of 7 : 3) for diagnosis and prognosis analyses. We subsequently used them to construct and validate the model. In the training group, we employed the Cox regression model to analyze the 11 predictors and eventually constructed a nomogram prediction model (Figure 3a) (Table 2). High APRI, poor classification of CTP, bad tumor grade/stage, HBV-DNA, portal hypertension, male, high total grade of ultrasonic enhancement, and high intensity of ultrasound enhancement at portal stage were considered risk factors associated with the risk of death. Earlier beginning time of ultrasonic contrast and high LMR were found to be protective factors in patients with HCC. We found that the calibration curve was in good agreement (Figure 3b), indicating that the model can predict OS of primary HCC. We also determined the time C index of each period (Figure 3c) and noted that OS models that combined ultrasound and clinical

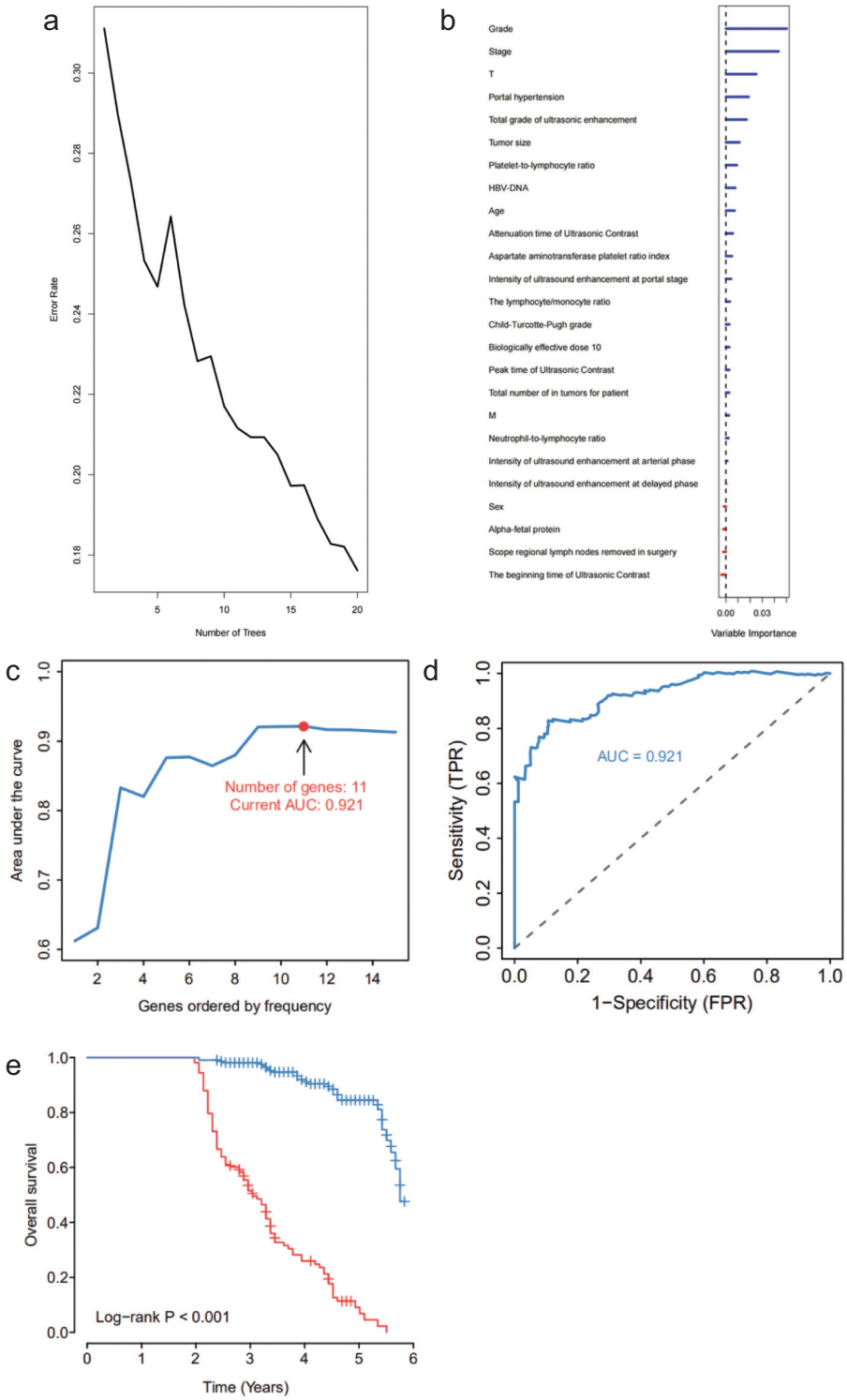

Figure 1. a-d. Feature extraction. Panel **(a)** shows the error rate for the data as a function of the classification tree. Panel **(b)** shows out-of-bag importance values for the predictors. Panel **(c)** shows random least absolute shrinkage and selection operator (LASSO) regressions and their incorporation into the Cox regression model according to the number of occurrences of predictors, followed by calculation of their area under the curve (AUC) values. This was performed to obtain the best combination of predictors. The receiver operating characteristic (ROC) curve **(d)** shows the accuracy of the prediction model based on 11 features (AUC = 0.921). In panel **(e)**, the Kaplan-Meier curves of factors selected using LASSO methods suggest the prediction model for the classification of poor survival rate patients based on the 11 characteristic factors ($P < .001$).

indicators exhibited better predictive capabilities. Finally, the AUC values of training and validation sets were 0.941 and 0.878, respectively (Figure 3d), reflecting that the built model showed excellent predicting ability.

Construction and verification of a nomogram for predicting PFS in primary hepatocellular carcinoma patients

To construct a nomogram for predicting PFS in primary HCC patients, we used LASSO-penalized multivariate Cox proportional hazards models to evaluate the characteristic factors. To obtain the best combination of predictors, we randomly executed 1000 LASSO regressions, then integrated them into the Cox regression model according to the number of occurrences of predictors, and eventually calculated their AUC values. Results indicated that incorporating the 11 predictive factors was effective in establishing the most effective prediction model (Figure 4a, 4b). Likewise, Kaplan-Meier curves revealed that the prediction model based on these 11 characteristic factors allowed accurate characterization of the poor survival rate of patients ($P < .001$) (Figure 4c). In the training set, the Cox model allowed analysis of these 11 predictors, hence, the construction of a nomogram prediction model (Figure 4d) (Table 3). High APRI, poor classification of CTP, bad tumor grade/stage, HBV-DNA, portal hypertension, male sex, high total grade of ultrasonic enhancement, and high intensity of ultrasound enhancement at portal stage were considered risk factors associated with the risk of recurrence. Earlier beginning time of ultrasonic contrast and high LMR were found to be protective factors in patients with HCC. Notably, the calibration curves of the prediction model showed a good agreement (Figure 4e), suggesting that the model can effectively predict the PFS of patients with primary HCC. Besides, we further performed a C index analysis in each period and found that PFS models that combined ultrasound and clinical indicators exhibited superior predictive capabilities (Figure 4f). Finally, the AUC values of training and validation sets in the prediction model were 0.795 and 0.719, respectively (Figure 4g), signifying that the PFS model possessed excellent predictive power.

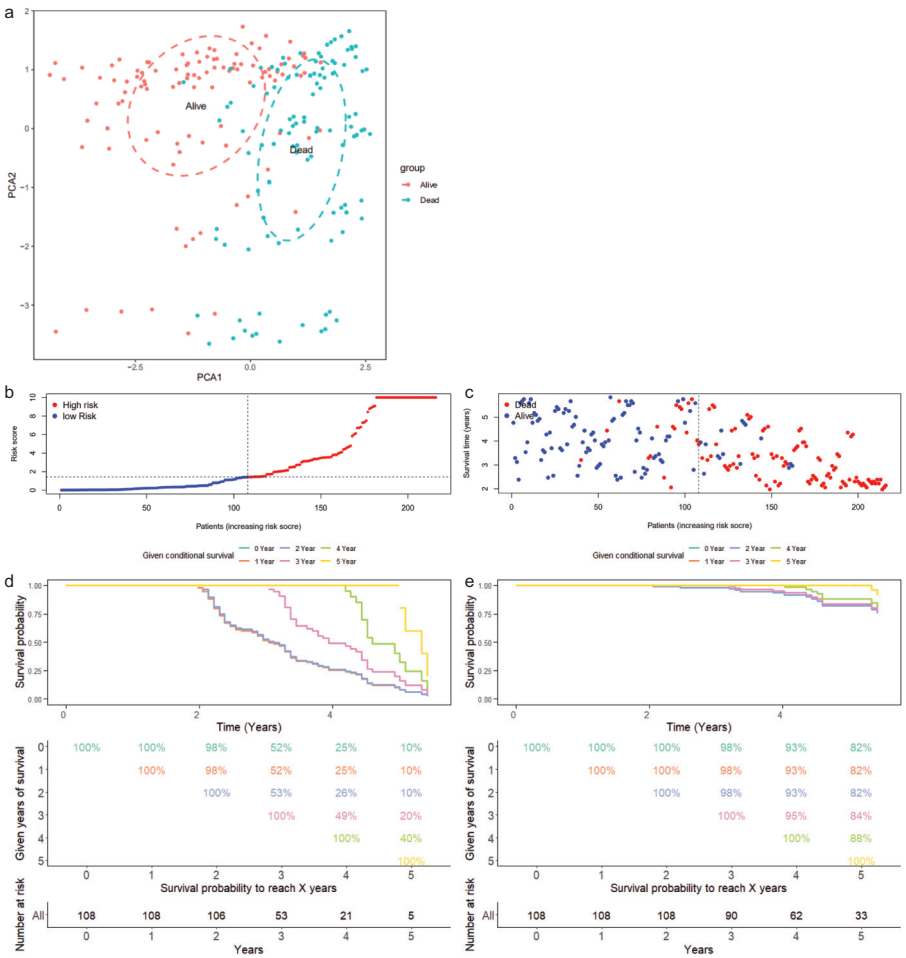

Figure 2. a-e. Characteristics of the 11 predictor factors and conditional survival. **(a)**, A principal component analysis (PCA) used to stratify the population and predict the survival rate of patients. *Blue* and *red* indicate dead and surviving subjects, respectively. Distribution of the risk score is based on 11 factors. Panel (**b**) shows classification of patients into different groups based on the risk score. **(c)**, Distribution of patient's prognosis and OS time. **(b-e)**, Kaplan-Meier estimates used to analyze conditional survival up to 5 years in 216 patients, given 0-5 years of survival in high/low-risk groups.

Figure 5 presents the results of the DCA of the models for predicting OS and PFS in patients with primary HCC. In general, we identified that the clinical decision-making of primary HCC based on the OS prediction and PFS prediction models could generate better benefits. This finding implies that these models are valuable in clinical practice and are therefore expected to ensure early prediction of OS and PFS in patients with primary HCC, thereby improving prognosis.

Discussion

To the best of our knowledge, this is the first study using easily available contrast-enhanced ultrasound indicators and clinical features to predict OS and PFS in HCC patients. In this work, we successfully built a prediction model and then verified its performance, including prediction accuracy, calibration, and clinical application, using an independent validation cohort. Overall, we found that a predictive model that combines contrast-enhanced ultrasound and clinical indicators exhibited superior predictive ability compared to the ones based on clinical indicators alone. APRI, CTP grade, tumor grade, HBV-DNA, the intensity of ultrasound enhancement at the portal stage, LMR, portal hypertension, sex, stage, the beginning time of ultrasonic contrast, and the total grade of ultrasonic enhancement were the major factors for the prognosis of liver cancer.

As the rapid development of artificial intelligence continues, the creation of diagnostic models for the disease may change the current paradigm of diagnosis and treatment, with many advances in this area already emerging.[27,28] Contrast-enhanced ultrasound examination is a newly developed technique that involves ultrasound examination-based technology. Functionally, it analyzes the blood flow of a patient by contrasting local lesions in the blood vessels,[29] thereby unraveling the pathological state and biological characteristics of tumor tissues. Previous studies have established that the analysis of blood flow in the tumor tissue is crucial to the evaluation of a patient's prognosis.[30–32] For PLC patients, an abnormal proliferation of blood vessels has been identified to cause a significant increase in the rate of local vascular malfo rmations.[33] Therefore, in the ultrasound examination, the smoothness of the blood flow and the blood perfusion volume of the patient's lesion is significantly increased, which has significant predictive value during the prognosis of the disease. The use of predictive models has been beneficial in more accurately driving diagnostic treatment choices for patients with HCC, particularly by simplifying the staging of the disease.[34,35] Hence, we believe that the development of a multimodal imaging histology prediction model could be a breakthrough in improving the diagnosis of HCC.

Findings from this study indicated that the intensity of the beginning time of ultrasonic contrast, ultrasound enhancement at the portal stage, and the total grade of ultrasonic enhancement were dominant risk factors for patient prognosis. First, the beginning time for ultrasonic contrast refers to the time when the contrast agent begins to diffuse into the patient's blood vessel. This primarily reflects the patency of the blood vessel in the patient's lesion and the pressure of the local blood vessel.[36] In general, the worse the condition of the liver, the later the ultrasound contrast agent would be started. This study found that the later the beginning of ultrasound contrast agent, the higher the risk of recurrence and the worse the prognosis of the patients. Second, the total grade of ultrasonic enhancement and the intensity of ultrasound enhancement at the portal stage also reflect the patency of the patient's blood vessels and the ability of collateral circulation. Specifically, it has been reported that a high total grade of ultrasonic enhancement and the intensity of ultrasound enhancement at the portal stage indicates that the patient has stronger

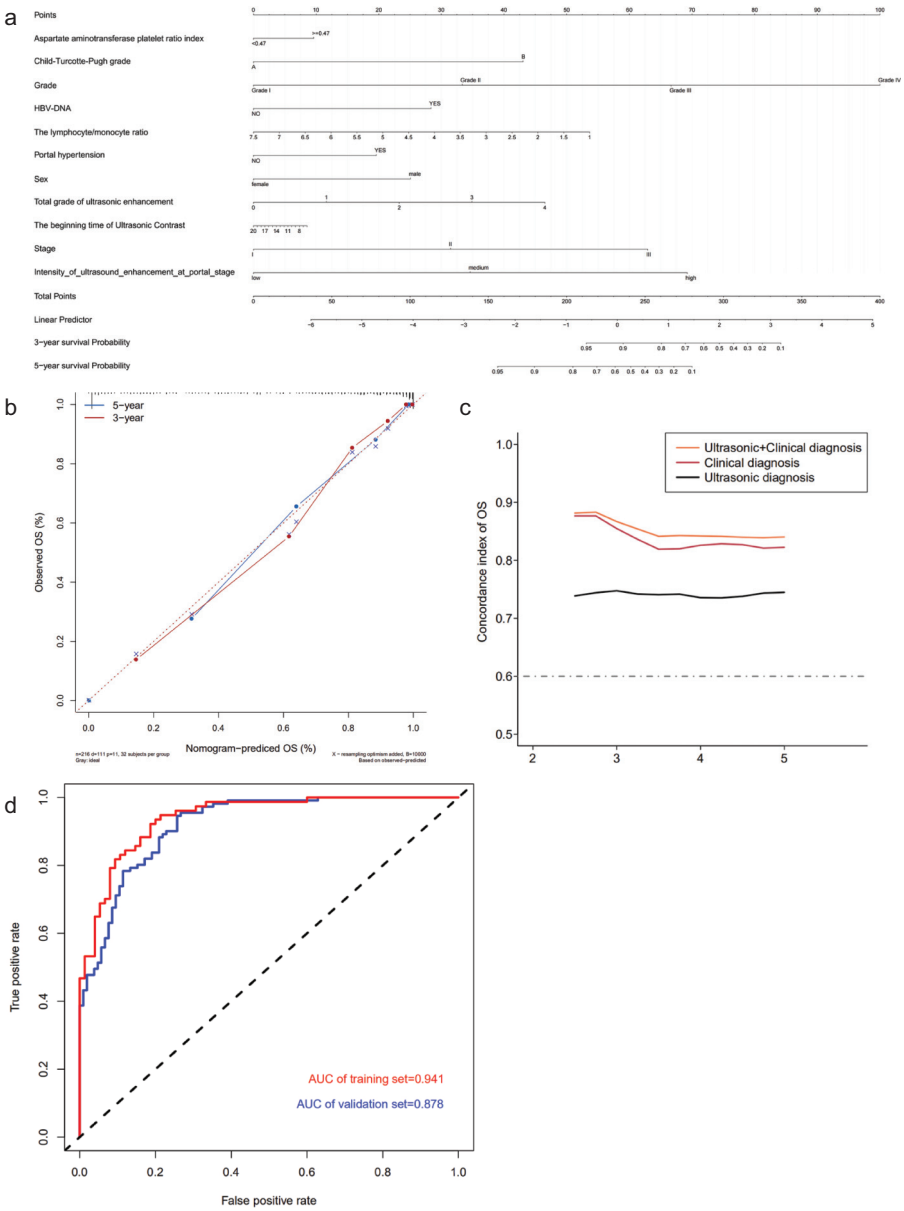

Figure 3. a-d. Construction of a personalized OS predictive model for patients with primary HCC. Panel **(a)** shows a model for predicting OS in patients with primary HCC. The model included APRI, CTP grade, tumor grade, HBV DNA, the intensity of ultrasound enhancement at the portal stage, LMR, portal hypertension, gender, stage, the beginning time of ultrasonic contrast, and total grade of ultrasonic enhancement. The nomogram for predicting OS in patients with HCC is shown in the figure. The first row in this panel is called points, which is the score reference for each variable. In the clinical treatment of a patient, we can calculate the scores of all predictor variables. Then, the total score can be mapped to the linear score linear predictor by total points to obtain the probability of OS for that patient. Panel **(b)** shows the nomogram calibration based on the primary HCC OS nomogram prediction model. Time C index **(c)** shows a measure of concordance of the predictor with OS in HCC patients. The ROC analysis **(d)** shows the predictive ability of the nomogram for predicting OS of primary HCC patients.

collateral circulation ability.[37] In general, well-differentiated tumors often take longer to enhance and subside to low enhancement because most of them still have a portal blood supply, while some lesions can show a certain degree of enhancement during the portal or delayed phases.[38] Some studies have reported that parameters of contrast-enhanced tumors are significantly associated with patient prognosis,[39] which was consistent with our findings. Therefore, a high total grade of ultrasonic enhancement and high intensity of ultrasound enhancement at portal phases were considered as risk factors associated with death and tumor recurrence.

In a Chinese study, patients with PLC were mostly infected with hepatitis, and their inflammatory state was implicated in promoting PLC development. NLR and APRI were found to effectively predict the prognosis of liver cancer.[40] Numerous reports have confirmed the involvement of inflammation in cancer pathogenesis and progression.[41] The occurrence of inflammation has been associated with the poor prognosis of multiple types of tumors.[42] Additionally, studies have highlighted that both NLR and APRI are sensitive indicators of the body's inflammatory system. These factors have been shown to reflect the inflammatory state and predict the prognosis of tumors, which agrees with our results.[43] Because of objective constraints, our study did not consider the possibility of patients being treated with direct-acting antiviral agents (DAA) during follow-up. Existing studies have not been able to determine the impact of DAA therapy on the incidence/recurrence of HCC in patients with viral hepatitis, and the debate on the impact of DAAs on the development of HCC is ongoing.[44] Thus, further cohort studies are required to verify the impact of DAA therapy on the prognosis of patients with HCC.

Previous studies have found that HBV-DNA is a risk marker for recurrence and death in HCC, while amplification of HBV-DNA affects the survival prognosis of patients with HCC. These findings are consistent with those of our study.[45] In addition, pathological/histological features are often a macroscopic composite of the tumor microenvironment, which is closely related to gene mutations.[46] Recent studies have also found that gene mutations can be identified by radiomics in some tumors.[47] For the aforementioned reasons, we formulated a hypothesis that diagnostic ultrasonography may also be able to identify mutational features of some genes, such as OATP1 or other mutations, as suggested by previous studies.[48] However, these conjectures are subject to further research in the future.

Of note, the innovation aspect of this work was in the ability to construct a model that effectively predicted OS and PFS of patients with primary HCC by combining easily available ultrasound indicators and clinical case characteristics. When compared to traditional models, our model does not require a computer for feature extraction. It is clinically applicable, with a strong

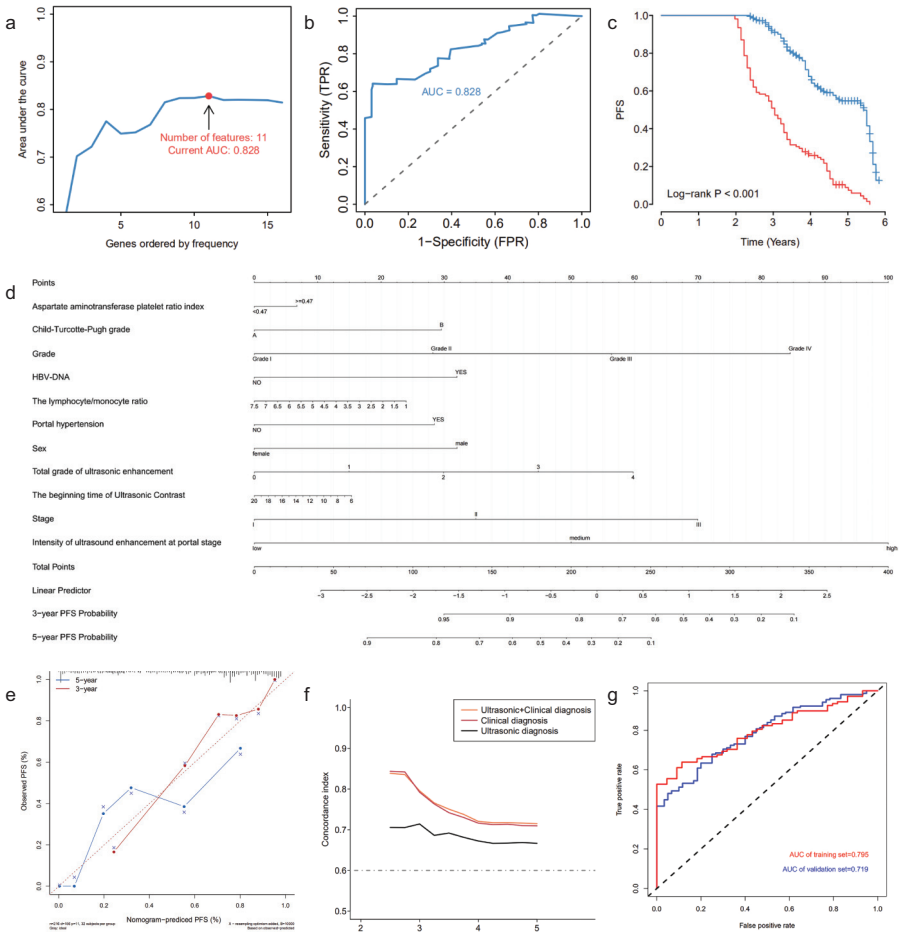

Figure 4. a-g. Construction of a personalized model for predicting PFS in primary HCC patients. Panel **(a)**: to obtain the best combination of predictors, we randomly performed 1000 LASSO regressions and incorporated them into the Cox regression model based on the number of occurrences of predictors. Their AUC values are also indicated.The ROC curve **(b)** shows the accuracy of the prediction model based on 11 features (AUC = 0.828). In panel **(c)**, Kaplan-Meier curves of factors selected using LASSO methods imply that the prediction model based on these 11 characteristic factors can accurately classify poor survival rates of patients ($P < .001$). Panel **(d)** shows a model for predicting PFS in patients with primary HCC. The model includes APRI, CTP grade, tumor grade, HBV DNA, the intensity of ultrasound enhancement at the portal stage, LMR, portal hypertension, gender, stage, the beginning time of ultrasonic contrast, and total grade of ultrasonic enhancement. The nomogram for predicting PFS in patients with HCC is shown in the figure. The first row in this panel is called points, which is the score reference for each variable. In the clinical treatment of a patient, we can calculate the scores of all predictor variables. Then, the total score can be mapped to the linear score linear predictor by total points to obtain the probability of PFS for that patient. Panel **(e)** shows nomogram calibration based on PFS nomogram prediction model for primary HCC. Time C index **(f)** shows a measure of concordance of the predictor with PFS in HCC patients. The ROC analysis **(g)** shows the predictive ability of the model for predicting PFS in primary HCC patients.

ability to better predict prognosis. Notably, early prediction of poor prognosis in patients will enable doctors and high-risk patients to better realize the importance of prognostic follow-up, hence improving this process. Thus, this prediction tool, developed herein, can further provide theoretical guidance for the clinical treatment and research of PLC patients.

During our analyses, all ultrasound examinations in patients were performed by experienced doctors, which eliminated bias caused by the differences in ultrasound diagnosis capabilities of different physicians. However, despite these promising results, this study also had some shortcomings. First, all patients in this cohort were from a single center. Therefore, further studies at multiple centers are needed to confirm our conclusions. Second, although our nomogram prediction model revealed good predictive stability and the model incorporating these current factors has the strongest predictive power, more data are still needed to validate the model. Clinical characteristics of HCC patients have to be considered important for predicting OS and PFS, such as sarcopenia.[49,50] For this reason, it may be necessary for us to incorporate sarcopenia or tumor size into our predictive models in the future. Additionally, we were unable to obtain all patient information because of permission restrictions. Thus, further research is required to expand the clinical information of patients. Third, we herein obtained data based on years of clinical history and past clinical work. Although the accuracy of these datasets is ensured, there is still a possibility of missing or incorrect information. Moreover, we recommended that a standardized evaluation method for contrast-enhanced ultrasound-related features is required. Although this simple method has been proven to achieve better predictive power, further research may be needed in the real world due to the difference in the equipments used. We excluded "patients who manifested severely inadequate heart, liver, and kidney functions; patients with other major diseases; and those with preoperative liver function of Child-Pugh C." The reason for this is that in our clinical practice, we find that these patients are more likely to die from noncancerous factors, thereby causing significant bias in the prediction model. Additionally, the blood indicators of these patients fluctuate considerably with the treatment cycle, such that the prediction model cannot be applied in these cases.

In conclusion, we have successfully built a model for predicting OS and PFS in primary HCC patients using easily available ultrasound indicators and clinical characteristics, including APRI, CTP grade, tumor grade, HBV-DNA, the intensity of ultrasound enhancement at the portal stage, LMR, portal hypertension, sex, stage, the beginning time of ultrasonic contrast, and the total grade of ultrasonic enhancement. The established model displayed excellent performance in terms of prediction accuracy, calibration, and clinical application, based on the results from the analysis of the validation cohort. We anticipate that this model will help clinicians to accurately predict poor prognosis in patients with HCC and ultimately improve the

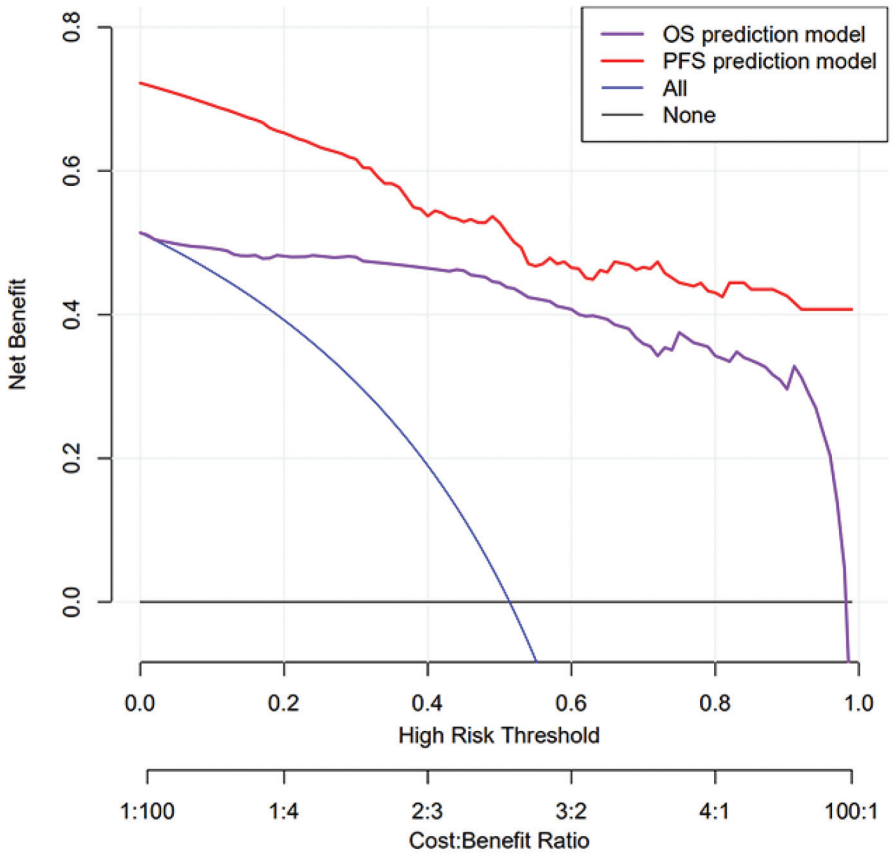

Figure 5. The decision curve analysis (DCA) curve for the estimation of OS and PFS.

postoperative prognosis. We also revealed that a predictive model that combines contrast-enhanced ultrasound and clinical indicators exhibited superior predictive ability compared to the one that uses clinical indicators alone.

Conflict of interest disclosure

The authors declared no conflicts of interest.

References

1. Losic B, Craig AJ, Villacorta-Martin C, et al. Intratumoral heterogeneity and clonal evolution in liver cancer. *Nat Commun*. 2020;11(1):291. [Crossref]
2. Scehnet JS, Jiang W, Kumar SR, et al. Inhibition of Dll4-mediated signaling induces proliferation of immature vessels and results in poor tissue perfusion. *Blood*. 2007;109(11):4753-4760. [Crossref]
3. Leem G, Chung MJ, Park JY, et al. Clinical value of contrast-enhanced harmonic endoscopic ultrasonography in the differential diagnosis of pancreatic and gallbladder masses. *Clin Endosc*. 2018;51(1):80-88. [Crossref]
4. Wu J, Chen DC. Contrast-enhanced ultrasonography: a promising method for blood flow and perfusion evaluation in critically ill patients. *Chin Med J (Engl)*. 2018;131(10):1135-1137. [Crossref]
5. Yao Z, Dong Y, Wu G, et al. Preoperative diagnosis and prediction of hepatocellular carcinoma: Radiomics analysis based on multi-modal ultrasound images. *BMC Cancer*. 2018;18(1):1089. [Crossref]
6. Chaturvedi AK, Caporaso NE, Katki HA, et al. C-reactive protein and risk of lung cancer. *J Clin Oncol*. 2010;28(16):2719-2726. [Crossref]
7. Elinav E, Nowarski R, Thaiss CA, Hu B, Jin C, Flavell RA. Inflammation-induced cancer: Crosstalk between tumours, immune cells and microorganisms. *Nat Rev Cancer*. 2013;13(11):759-771. [Crossref]
8. Antonioli L, Blandizzi C, Pacher P, Haskó G. Immunity, inflammation and cancer: A leading role for adenosine. *Nat Rev Cancer*. 2013;13(12):842-857. [Crossref]
9. Marasco G, Colecchia A, Silva G, et al. Non-invasive tests for the prediction of primary hepatocellular carcinoma. *World J Gastroenterol*. 2020;26(24):3326-3343. [Crossref]
10. Marasco G, Colecchia A, Colli A, et al. Role of liver and spleen stiffness in predicting the recurrence of hepatocellular carcinoma after resection. *J Hepatol*. 2019;70(3):440-448. [Crossref]
11. Leoni S, Piscaglia F, Granito A, et al. Characterization of primary and recurrent nodules in liver cirrhosis using contrast-enhanced ultrasound: Which vascular criteria should be adopted? *Ultraschall Med*. 2013;34(3):280-287. [Crossref]
12. Claudon M, Cosgrove D, Albrecht T, et al. Guidelines and good clinical practice recommendations for contrast enhanced ultrasound (CEUS)—update 2008. *Ultraschall Med*. 2008;29(1):28-44. [Crossref]
13. Bruix J, Sherman M. Management of hepatocellular carcinoma. *Hepatology*. 2005;42(5):1208-1236.
14. YZ. The relationship between contrast-enhanced ultrasonographicenhanced intensity and microvessel density of gastric cancer. *Journal of Logistics University of CAPF (Medical Sciences)*. 2012;21:604-607.
15. Friedman J, Hastie T, Tibshirani R. Regularization paths for generalized linear models via coordinate descent. *J Stat Softw*. 2010;33(1):1-22. [Crossref]
16. Sauerbrei W, Royston P, Binder H. Selection of important variables and determination of functional form for continuous predictors in multivariable model building. *Stat Med*. 2007;26(30):5512-5528. [Crossref]
17. Kidd AC, McGettrick M, Tsim S, Halligan DL, Bylesjo M, Blyth KG. Survival prediction in mesothelioma using a scalable LASSO regression model: Instructions for use and initial performance using clinical predictors. *BMJ Open Respir Res*. 2018;5(1):e000240. [Crossref]
18. Sveen A, Ågesen TH, Nesbakken A, et al. ColoGuidePro: A prognostic 7-gene expression signature for stage III colorectal cancer patients. *Clin Cancer Res*. 2012;18(21):6001-6010. [Crossref]
19. Hu M, Zhong X, Cui X, et al. Development and validation of a risk-prediction nomogram for patients with ureteral calculi associated with urosepsis: A retrospective analysis. *PLoS One*. 2018;13(8):e0201515. [Crossref]
20. Chen YS, Cai YX, Kang XR, et al. Predicting the risk of sarcopenia in elderly patients with patellar fracture: Development and assessment of a new predictive nomogram. *PeerJ*. 2020;8:e8793. [Crossref]
21. Iasonos A, Schrag D, Raj GV, Panageas KS. How to build and interpret a nomogram for cancer prognosis. *J Clin Oncol*. 2008;26(8):1364-1370. [Crossref]
22. Balachandran VP, Gonen M, Smith JJ, DeMatteo RP. Nomograms in oncology: More than meets the eye. *Lancet Oncol*. 2015;16(4):e173-e180. [Crossref]
23. Kramer AA, Zimmerman JE. Assessing the calibration of mortality benchmarks in critical care: The Hosmer-Lemeshow test revisited. *Crit Care Med*. 2007;35(9):2052-2056. [Crossref]
24. Pencina MJ, D'Agostino RB. Overall C as a measure of discrimination in survival analysis: Model specific population value and confidence interval estimation. *Stat Med*. 2004;23(13):2109-2123. [Crossref]
25. Van Calster B, Wynants L, Verbeek JFM, et al. Reporting and interpreting decision curve analysis: A guide for investigators. *Eur Urol*. 2018;74(6):796-804. [Crossref]
26. Collins GS, Reitsma JB, Altman DG, Moons KG. Transparent reporting of a multivariable prediction model for individual prognosis or diagnosis (TRIPOD): The TRIPOD statement. *BMJ*. 2015;350:g7594. [Crossref]

27. Kang XR, Chen B, Chen YS, et al. A prediction modeling based on SNOT-22 score for endoscopic nasal septoplasty: A retrospective study. *PeerJ*. 2020;8:e9890. [Crossref]
28. Peng J, Zhang J, Zhang Q, Xu Y, Zhou J, Liu L. A radiomics nomogram for preoperative prediction of microvascular invasion risk in hepatitis B virus-related hepatocellular carcinoma. *Diagn Interv Radiol*. 2018;24(3):121-127. [Crossref]
29. Shiozawa K, Watanabe M, Ikehara T, et al. Efficacy of intra-arterial contrast-enhanced ultrasonography during transarterial chemo embolization with drug-eluting beads for hepatocellular carcinoma. *World J Hepatol*. 2018;10(1):95-104. [Crossref]
30. Kim HS, Moon JH, Lee YN, et al. Prospective comparison of intraductal ultrasonogr aphy-guided transpapillary biopsy and conventional biopsy on fluoroscopy in suspected malignant biliary strictures. *Gut Liver*. 2018;12 (4):463-470. [Crossref]
31. Yokode M, Shiomi H, Itai R, et al. [Diagnostic utility of endoscopic ultrasonography elastography and contrast-enhanced harmonic endoscopic ultrasonography in a patient with type 2 autoimmune pancreatitis]. *Nihon Shokakibyo Gakkai Zasshi*. 2018;115(6):563-572.
32. Lee TH. Can contrast-enhanced harmonic endoscopic ultrasonography differentiate malignancy from benign disease? *Clin Endosc*. 2018;51(1):5-7. [Crossref]
33. Shi XC, Tang SS, Zhao W. Contrast-enhanced ultrasound imaging characteristics of malignant transformation of a localized type gallbladder adenomyomatosis: A case report and literature review. *J Cancer Res Ther*. 2018;14(Supplement): S263-s266. [Crossref]
34. Giannini EG, Moscatelli A, Pellegatta G, et al. Application of the intermediate-stage subclassification to patients with untreated hepatocellular carcinoma. *Am J Gastroenterol*. 2016;111(1):70-77. [Crossref]
35. Vasuri F, Renzulli M, Fittipaldi S, et al. Pathobiological and radiological approach for hepatocellular carcinoma subclassification. *Sci Rep*. 2019;9:14749. [Crossref]
36. Huang M, Zhao Q, Chen F, You Q, Jiang T. Atypical appearance of hepatic hemangiomas with contrast-enhanced ultrasound. *Oncotarget*. 2018;9(16):12662-12670. [Crossref]
37. Cui G, Martin RC, Liu X, et al. Serological biomarkers associate ultrasound characteristics of steatohepatitis in mice with liver cancer. *Nutr Metab (Lond)*. 2018;15:71. [Crossref]
38. Sun MRM, Ngo L, Genega EM, et al. Renal cell carcinoma: Dynamic contrast-enhanced MR imaging for differentiation of tumor subtypes —Correlation with pathologic findings. *Radiology*. 2009;250(3):793-802. [Crossref]
39. Nuciforo S, Fofana I, Matter MS, et al. Organoid models of human liver cancers derived from tumor needle biopsies. *Cell Rep*. 2018;24 (5):1363-1376. [Crossref]
40. Lu SD, Wang YY, Peng NF, et al. Preoperative ratio of neutrophils to lymphocytes predicts postresection survival in selected patients with early or intermediate stage hepatocellular carcinoma. *Medicine (Baltimore)*. 2016;95(5):e2722. [Crossref]
41. Sanford DE, Belt BA, Panni RZ, et al. Inflammatory monocyte mobilization decreases patient survival in pancreatic cancer: A role for targeting the CCL2/CCR2 axis. *Clin Cancer Res*. 2013;19(13):3404-3415. [Crossref]
42. Pribluda A, Elyada E, Wiener Z, et al. A senescence-inflammatory switch from cancer-inhibitory to cancer-promoting mechanism. *Cancer Cell*. 2013;24(2):242-256. [Crossref]
43. Wang D, Bai N, Hu X, et al. Preoperative inflammatory markers of NLR and PLR as indicators of poor prognosis in resectable HCC. *PeerJ*. 2019;7:e7132. [Crossref]
44. Guarino M, Sessa A, Cossiga V, Morando F, Caporaso N, Morisco F. Direct-acting antivirals and hepatocellular carcinoma in chronic hepatitis C: A few lights and many shadows. *World J Gastroenterol*. 2018;24 (24):2582-2595. [Crossref]
45. Witjes CD, IJzermans JN, Van Der Eijk AA, Hansen BE, Verhoef C, De Man RA. Quantitative HBV DNA and AST are strong predictors for survival after HCC detection in chronic HBV patients. *Neth J Med*. 2011;69 (11):508-513.
46. Lendvai G, Szekerczés T, Illyés I, et al. Cholangiocarcinoma: Classification, histopathology and molecular carcinogen esis. *Pathol Oncol Res*. 2020;26(1):3-15. [Crossref]
47. Pinker K, Shitano F, Sala E, et al. Background, current role, and potential applications of radiogenomics. *J Magn Reson Imaging*. 2018;47(3):604-620. [Crossref]
48. Vasuri F, Golfieri R, Fiorentino M, et al. OATP 1B1/1B3 expression in hepatocellular carcinomas treated with orthotopic liver transplantation. *Virchows Arch*. 2011;459(2): 141-146. [Crossref]
49. Marasco G, Serenari M, Renzulli M, et al. Clinical impact of sarcopenia assessment in patients with hepatocellular carcinoma undergoing treatments. *J Gastroenterol*. 2020;55(10):927-943. [Crossref]
50. Marasco G, Dajti E, Ravaioli F, et al. Clinical impact of sarcopenia assessment in patients with liver cirrhosis. *Expert Rev Gastroenterol Hepatol*. 2021;15(4):377-388. [Crossref]